ACS APPLIED MATERIALS & INTERFACES

www.acsami.org

Research Article

High Refractive Index Photopolymers by Thiol−Yne "Click" Polymerization

Sudheendran Mavila, Jasmine Sinha, Yunfeng Hu, Maciej Podgórski, Parag K. Shah, and Christopher N. Bowman*

Cite This: *ACS Appl. Mater. Interfaces* 2021, 13, 15647−15658

Read Online

ACCESS | Metrics & More | Article Recommendations | Supporting Information

ABSTRACT: A scalable synthesis of high refractive index, optically transparent photopolymers from a family of low-viscosity multifunctional thiol and alkyne monomers via thiol−yne "click" is described herein. The monomers designed to incorporate high refractive index cores consisting of aryl and sulfide groups with high intrinsic molar refraction were synthesized starting from commercially available low-cost raw materials. The low-viscosity (<500 cP) thiol−yne resins formulated with these new multifunctional monomers and a phosphine oxide photoinitiator underwent efficient thiol−yne polymerizations upon exposure to 405 nm light at 30 mW/cm^2. In contrast to the previously reported thiol−ene systems, the kinetic profile of these photopolymerizations showed significant dependence on the nature of the thiol and alkyne monomers. However, the ability of the thiol−yne reaction to introduce a large number of sulfide linkages compared to that of thiol−ene systems yielded cross-linked high optical quality photopolymers with a polymer refractive index that exceeds 1.68 (n_D/20 °C). Interestingly, the photopolymer formed from the least sterically hindered alkynyl thioether monomer **2b** with flexible thioether core and the dithiol **1a** exhibited unprecedented difference in the polymer refractive index as compared to that of the resin with polymerization-induced changes reaching up to 0.08. Furthermore, the implementation of these low-viscosity thiol−yne resins was demonstrated by preparing two-stage photopolymeric holographic materials with a dynamic range of ∼0.02 and haze < 1.5% in two-dimensional high refractive index structures.

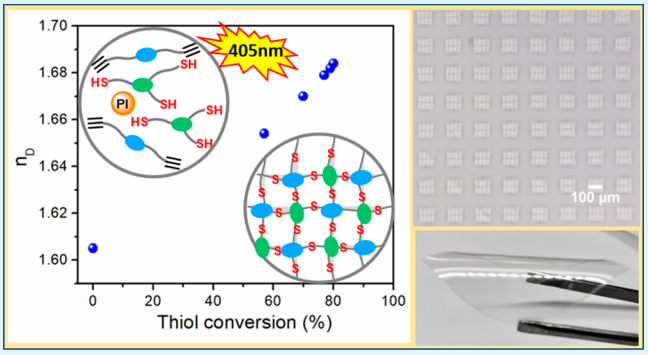

KEYWORDS: *thiol−yne click chemistry, photopolymer, holography, high Δn, high refractive index structures*

INTRODUCTION

High refractive index polymers (HRIPs) are recognized as an interesting alternative to silicon and glasses for various optoelectronic applications because of their lightweight, ease of processability, low cost, and versatility in control over material properties.[1−4] In recent years, HRIPs gained increasing interest because of their potential applications in lenses, antireflective coatings, optical adhesives, and other optical materials.[5,6] In general, there are two ways to achieve high refractive indices in these polymers: (1) By introducing atoms or groups with high intrinsic molar refractions or (2) by introducing high refractive index inorganic nanoparticles in the polymer matrix. Thus, efforts to improve the refractive indices of these materials mainly focused on introducing groups or atoms with high molar refraction.[7] While significant progress has been made in the development of intrinsic HRIPs, the majority of these strategies rely on thermally driven polymerization techniques that suffer from a lack of optical transparency and spatial and temporal control.[8−13] However, to achieve high performance in various applications including additive manufacturing,[14,15] GRIN optics,[16] and HOEs,[17,18] polymers with refractive indices ranging from 1.3 to >1.6 are highly desirable. The design and synthesis of such high-performance HRIP materials require the use of the best available organic and polymer synthetic strategies such as thiol-X "click" chemistry. Rapid and efficient thiol-X photopolymerizations allow for the uniform incorporation of a large number of sulfide linkages that possess high intrinsic molar refraction throughout the polymer network.[19−23] Thus, the sulfur content and cross-link density of the network polymer are easily tuned with a strong correlation existing between the sulfur content and the network refractive index. Furthermore, the step-growth mechanism leads to the formation of a polymer network with low intrinsic shrinkage stress[24,25] with minimum leachable monomers and exceptional

Received: January 15, 2021
Accepted: March 17, 2021
Published: March 29, 2021

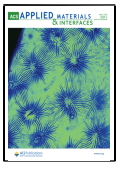

resistance to oxygen inhibition.[22] In combination with sulfur, phosphorus also has been used to improve the refractive index further.[26] However, most of the commercially available monomers for thiol-X networks are either expensive with limited availability or low in refractive indices because of the presence of additional groups with low molar refraction. While there exist several reports on monomer designs that are capable of achieving refractive index values > 1.6, these monomer designs are highly restrictive with respect to the consideration of other important material properties, solubility, and other characteristics. Recently, to address the deficiency in photopolymerizable high refractive index monomers, Bowman and co-workers developed a scalable and highly modular synthetic strategy to produce multifunctional thiol and ene monomers in relatively large scale using inexpensive, widely available raw materials.[27] All of those synthesized low-viscosity (<500 cP) monomers possessed refractive index values (n_D) > 1.6, exhibited excellent resin solubility, and were photopolymerized under ambient conditions upon irradiating with 405 nm LED irradiation at 10 mW/cm^2 for 10 s.

A further increase in the refractive index and cross-linking density of the network polymers without altering the molecular weight or core structure of the monomer is quite challenging. To this end, Hoyle and co-workers demonstrated the importance of thiol−yne "click" photopolymerization to increase the polymer refractive indices going up to as high as 1.66.[28,29] This significant increase in the refractive index of the thiol−yne photopolymer is attributed to their ability to incorporate a larger concentration of sulfide linkages as compared to the analogous radical-mediated thiol−ene system. Mechanistically, in thiol−yne reactions, up to two thiol groups are added to a single alkyne group via a two-step process involving the formation of a vinyl sulfide intermediate. Bowman and co-workers explored the kinetics and mechanism of these highly cross-linked thiol−yne photopolymers employing various commercially available multifunctional thiols and alkyne monomers.[30−32]

In general, thiol−yne reactions are performed by three different methods including free radical reactions and amine-mediated and transition metal catalysis.[33,34] Due to their ability to introduce a large number of functionalities with minimal byproducts, thiol−yne polymerizations have been used in the formation of hyperbranched polymers and dendrimers for use in drug delivery applications and recently as an antimicrobial wound dressing material.[35−38] Meanwhile, it has also been reported that the reaction of aromatic alkynes and thiols yields only monoaddition products resulting in the formation of polyvinyl sulfides.[39] Although there exist scattered recent reports on thiol−yne-based photopolymers, far fewer applications and studies have, however, been directed toward scalable synthesis of high refractive index monomers and photopolymers. On the basis of the general synthetic protocol developed for high RI thiol−yne photopolymers, here, a set of high refractive index, low-viscosity propargyl ethers is reported that form miscible resins with multifunctional thiols. Photopolymerization of these resin mixtures under mild conditions results in optically transparent films with refractive index values (n_D) ranging from 1.63 to 1.69.

EXPERIMENTAL SECTION

Materials. All of the following chemicals were purchased and used as received. Thiophenol, epichlorohydrin, and butylated hydroxytoluene (BHT) were purchased from Alfa Aesar. Bis(2-mercaptoethyl sulfide (**1a**) and diphenyl (2,4,6-trimethylbenzoyl)phosphineoxide (TPO) were purchased from TCI America. Thiourea, propargyl bromide (80% solution in toluene), triethylamine (Et_3N), 2-mercaptoethanol, and sodium hydride were purchased from Sigma-Aldrich. 1,8-Diazabicyclo[5.4.0]undec-7-ene (DBU) was purchased from Chem-Impex International. Syntheses of **1b**, **1c**, **BPTP**, **EDTOH**, and **TBTOH** were adapted from previously reported procedures in the literature.[27] A detailed synthetic procedure can be found in the Supporting Information.

Synthesis of 3,3′-[Thiobis(2,1-ethanediylthio)]bis[1-propyne] (2b). To a 250 mL round-bottomed flask equipped with a magnetic stir bar was added 6.5 g (116.6 mmol, 3.6 equiv) of KOH and was dissolved in 15 mL of methanol. The flask was then was purged with argon for 10 min to eliminate any oxygen and then cooled to 0 °C. To this was added 5.0 g (32.4 mmol, 1 equiv) of **1a** dissolved in 10 mL of methanol dropwise under inert atmosphere. After 5 min of stirring at 0 °C, a solution of 8.7 g (116.6 mmol, 3.6 equiv) of propargyl chloride dissolved in 10 mL of methanol was added dropwise and stirred at room temperature for another 12 h. After this period, the precipitated KCl was filtered off, and the filtrate was evaporated under reduced pressure to remove all of the volatiles. The residue obtained was diluted with 250 mL of CH_2Cl_2, transferred to a separatory funnel, washed with water (2 × 50 mL) and brine (1 × 50 mL), dried over anhydrous Na_2SO_4, filtered, and evaporated under reduced pressure to obtain the crude product as a pale yellow liquid which was purified by silica-gel column chromatography using 10% EtOAc/hexanes as eluent to yield 6.4 g (85%) of the title compound **2b** as a colorless oil which was solidified upon standing. ^{1}H NMR (400 MHz, $CDCl_3$): δ = 3.31 (d, J = 2.6 Hz, 1H), 2.97−2.89 (m, 1H), 2.86−2.79 (m, 1H), 2.28 (t, J = 2.6 Hz, 1H). ^{13}C NMR (101 MHz, $CDCl_3$): δ = 79.7, 71.7, 31.6, 19.4.

General Procedure for the Synthesis of Propargyl Ether Monomers. Monomers **2a**, **2c**, and **2d** were synthesized following a similar procedure previously reported.[27] Briefly, to a round-bottomed flask equipped with a magnetic stir bar, the corresponding alcohol (1 equiv) was dissolved in anhydrous THF (0.2 M, with respect to alcohol) and cooled to 0 °C, and sodium hydride (1.5 equiv) was added in portions under N_2 atmosphere. After stirring at 0 °C for 30 min, propargyl bromide (1.5 equiv with respect to the hydroxyl group, 80% solution in toluene) was added dropwise at 0 °C followed by addition of a catalytic amount of potassium iodide. The reaction vessel was allowed to stir at room temperature for 16 h. After this period, consumption of the starting materials was monitored by TLC, and the volatiles were removed under reduced pressure. The residue was diluted with EtOAc, washed with 1 N HCl, water, and brine, dried over anhydrous sodium sulfate, and filtered. The filtrate was evaporated under reduced pressure to yield the crude product, which was purified by silica-gel column chromatography using 30% EtOAc/hexanes as eluent to yield the title compound.

*1,3-Bis(phenylthio)-2-propane Propargyl Ether (**2a**).* Pale yellow liquid; 91% yield. ^{1}H NMR (400 MHz, $CDCl_3$): δ 7.36−7.33 (m, 4H), 7.28−7.24 (m, 4H), 7.20−7.16 (m, 2H), 4.21 (d, J = 2.4 Hz, 2H), 3.87 (p, J = 5.9 Hz, 1H), 3.23 (dd, J = 5.9, 1.7 Hz, 4H), 2.36 (t, J = 2.4 Hz, 1H). ^{13}C NMR (101 MHz, $CDCl_3$, 25 °C): δ 136.0, 129.7, 129.1, 126.4, 79.6, 76.7, 74.9, 57.6, 37.2.

*1, 2-Ethanedithiol-Based Dipropargyl Ether (**2c**).* Pale yellow liquid, 66% yield. ^{1}H NMR (400 MHz, $CDCl_3$): δ 7.40−7.38 (m, 4H), 7.31−7.26 (m, 4H), 7.21−7.19 (m, 2H), 4.25 (d, J = 2.5 Hz, 4H), 3.88−3.82 (m, 2H), 3.22 (dd, J = 5.9, 1.2 Hz, 4H), 2.90−2.79 (m, 4H), 2.75 (s, 4H), 2.42 (td, J = 2.4, 0.7 Hz, 2H). ^{13}C NMR (101 MHz, $CDCl_3$, 25 °C): δ 136.0, 129.6, 129.2, 126.5, 79.7, 77.5, 75.1, 57.5, 36.8, 35.3, 33.1.

*4, 4′-Thiobisbenzenethiol-Based Dipropargyl Ether (**2d**).* Pale yellow liquid; 76% yield. ^{1}H NMR (400 MHz, $CDCl_3$): δ 7.36−7.34 (m, 4H), 7.28−7.24 (m, 8H), 7.21−7.18 (m, 6H), 4.22 (d, J = 2.4 Hz, 4H), 3.94−3.78 (m, 2H), 3.24−3.20 (m, 8H), 2.36 (td, J = 2.4, 0.5 Hz, 2H). ^{13}C NMR (101 MHz, $CDCl_3$, 25 °C): δ 135.8, 135.5, 133.5, 131.6, 130.1, 129.7, 129.2, 126.5, 79.6, 76.6, 75.1, 57.6, 37.1.

Nuclear Magnetic Resonance (NMR). All ^{1}H NMR(400 MHz) and ^{13}C NMR (101 MHz) spectra were recorded in $CDCl_3$ on a

https://doi.org/10.1021/acsami.1c00831
ACS Appl. Mater. Interfaces 2021, 13, 15647−15658

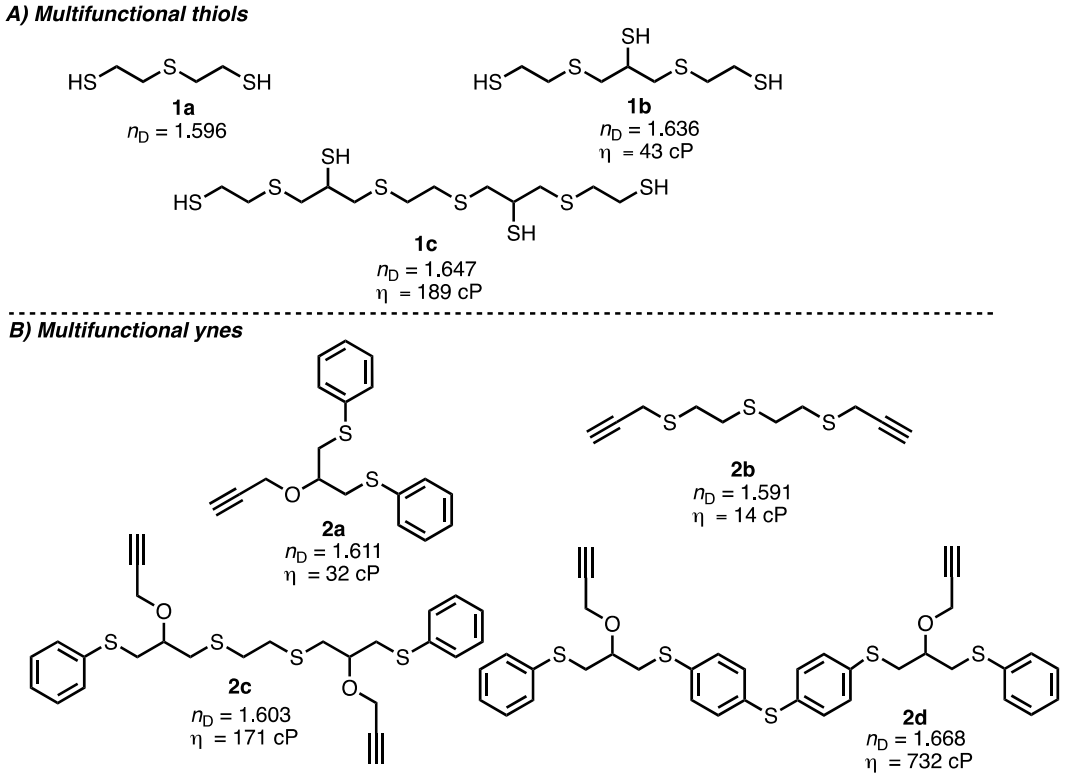

Figure 1. Structure of high refractive index multifunctional thiols (A) and alkynes (B) used in this study along with their measured viscosity and refractive index (nD/20 °C) values.

Bruker AVANCE-III 400 NMR spectrometer. All of the chemical shifts are reported in ppm relative to the residual chloroform solvent peak (δ = 7.26 ppm, ^{1}H and δ = 77.00 ppm, ^{13}C) as the internal standard.

Fourier Transform Infrared Spectroscopy (FTIR). Thiol−yne polymerization kinetics were analyzed using a Nicolet 8700 FTIR spectrometer in transmission mode as reported earlier.[27] Irradiation was performed using a 405 nm LED light source (Thorlabs) at an intensity of 30 mW/cm^2 after 1 min and continued for 10 min. The real-time thiol conversion (c-thiol) and alkyne conversion (c-alkyne) were monitored using a series scan, integrating over the ranges 2550−2600 and 2150−2150 cm^{-1}, respectively. Conversion of functional groups (c) was calculated with the equation

$$c = (1 - A/A_{initial}) \times 100\% \quad (1)$$

where $A_{initial}$ is the area of the unconsumed functional group peak and A is the area under the thiol or C≡C peak after the thiol−yne reaction.

Refractive Index Measurements. A digital refractometer (Abbemat MW) was used to measure refractive index values at 20 °C at the Fraunhofer lines—sodium-D (589 nm).

Viscosity Measurement. The viscosities of the liquid monomers were obtained using a rotational rheometer (ARES-G2, TA Instruments) operating in a parallel plate geometry using a 0.4 mm gap at a shear rate of 600 s^{-1} using 20 mm diameter quartz plates at ambient temperature. All resins exhibited Newtonian fluid behavior.

Dynamic Mechanical Analysis (DMA). A DMA (Q800, TA Instruments) was used to conduct temperature sweep experiments on rectangular photopolymer films with an applied oscillatory strain of 0.1%. Sample dimensions were approximately 10 × 5 × 0.5 mm. A temperature ramp rate of 3 °C/min was used from −30 to 60 °C at a frequency of 1 Hz. The glass transition temperature (T_g) was taken as the peak of the tan δ curve. The glass transition temperature (T_g) and melting temperature (T_m) of polymers with low cross-link densities were measured by differential scanning calorimetry (DSC) on a DSC 2500 (TA Instruments) with a heating rate of 5 °C/min.

Film Preparation for Hologram Recording. Two-stage photopolymer systems containing linear polyurethane binder and the high RI monomers were prepared as per the previously published procedure.[45] Briefly, a mixture of 1.4 g of polycaprolactone-*b*-polytetrahydrofuran-*block*-polycaprolactone ($M_n \approx 2000$), 0.168 g of 1,6-diisocyanatohexane, and 0.052 g of 2-(allyloxymethyl)-2-ethyl-1,3-propanediol (for 30% pendent allyl groups) was thermally cured at 70 °C overnight. After this period, a stock solution of the linear polyurethane was prepared by dissolving the polymer in 9.2 g of acetone. In another 20 mL drum vial, a stoichiometric mixture of 0.15 g of thiol−yne writing monomers (TMPTMP and a high RI yne monomer **2a**, **2c**, or **2d**) was mixed with 1.33 g of the linear polyurethane stock solution followed by 3 wt % of TPO. A 200 μL amount of this resin mixture was withdrawn and blade coated at 50 °C on a Fisher Brand 2.54 cm × 7.62 cm glass slide using a ZAA 2300 Automatic Film Applicator to obtain ∼10 μm thick samples.

Holographic Recording. Transmission holograms were recorded in a two-beam interference setup according to previously published procedures (see the Supporting Information for a detailed procedure).[17,45]

Haze Measurement of the Recorded Hologram. The haze measurement of the flood-cured samples was obtained using a Haze-gard i haze meter from BYK that has a measuring area of ø 18 mm. The average haze and the standard deviation were calculated from the haze measured at three different spots on the sample.

Two-Stage Photomask Exposure. A two-stage photopolymer system consisting of poly(urethanethiourethane) and thiol−yne resin was prepared by mixing high refractive index thiol **1b** and diyne **2b** (35 wt %) with low refractive index TNCO and TMPTG (65 wt %) along with 2 wt % of TPO. Thiols and yne were mixed first, and then TNCO was added. A well-mixed, homogeneous resin was casted between a pair of clean glass slides (Fisher Scientific) using 250 μm thick spacers (Precision Brand) to control film thickness. The samples were cured (stage 1 reaction) at ambient temperature for 30 min. Stage 2 recording was performed using a standard black and white transparency-based photomask and a 30 s irradiation with a 405 nm LED source (50 mW/cm^2). Matrix refractive index (n_D) = 1.5427.

https://doi.org/10.1021/acsami.1c00831
ACS Appl. Mater. Interfaces 2021, 13, 15647−15658

Mechanical Tensile Testing. Uniaxial tensile tests were performed using an Exceed model E42, 500 N load cell (MTS Systems Corp.) on rectangular samples cut from bulk films with thicknesses of ~250 μm. The samples were strained at 10 mm/min at ambient temperature.

Ultraviolet−Visible (UV−vis). Optical transmittance of the photopolymers was measured on an Evolution 300 UV−vis (Thermo Scientific) from 400 to 1000 nm through 250 μm thick films at a scanning speed of 60 nm min^{-1}.

RESULTS AND DISCUSSION

Structure and Synthesis of High Refractive Index Thiols and Alkyne Monomers. A thoughtful utilization of various thiol-X click reactions in monomer synthesis not only allows for the incorporation of a high number of sulfide groups but also results in the reaction having high yields with minimal side products. On the basis of the recently developed scalable strategy, all of the monomers discussed here are synthesized starting from inexpensive and widely available raw materials and employ efficient utilization of thiol−epoxide and thiol−halide click reactions (Scheme S1).[27] The general strategy developed here also provides a high degree of freedom over the choice of the backbone and polymerizable pendent groups. As can be seen from Figure 1, the structure of each monomer differs in its core structure and the nature and position of the reactive functionalities. For example, the simplest yne monomer **2a** only forms low cross-link density polymers as there is only one alkynal group but possesses low viscosity (32 cP) and high n (1.611) compared to the rest of the aryl-containing monomers **2c** and **2d**. The diyne monomer **2b** has completely different structural features from the rest of the yne monomers as this monomer has only sulfur in its backbone and no aryl groups. Though the refractive index is low (1.591), this monomer is sterically the least hindered and has the primary thiopropargyl functionality. Similarly, as we go from **1a** to **1c** in thiol monomers, the number of secondary thiol groups increases along with a corresponding increase in the refractive index. Specific material properties such as T_g, modulus, and hydrophobicity are easily tuned while maintaining a flexibility of the backbone with enhanced solubility. For example, flexible sulfide linkages throughout the monomer design facilitate a refractive index increase without sacrificing the initial resin viscosity, solubility, or other optically desirable characteristics of a given monomer/resin.

As the minimum thiol functionality required to form a linear polymer via a thiol−yne click reaction is two, commercially available 2,2′-thiodiethanethiol (**1a**) with a refractive index (nD/20 °C) of 1.596 was used as the simplest dithiol. The trithiol (**1b**) and tetrathiol (**1c**) were obtained following the previous procedure starting from the ring-opening reaction of epichlorohydrin with 2-mercaptoethanol under mild reaction conditions.[27] In this manner, the reaction of 1 equiv of 2-mercaptoethanol with epichlorohydrin in the presence of a catalytic amount of borax quantitatively and selectively yielded the monosubstituted product 1-chloro-3-(phenylthio)-2-propanol (**CPTP**), which was further reacted with 0.5 equiv of ethane dithiol to give the corresponding tetrahydroxy intermediate (**TetraOH**). Similarly, the trihydroxy intermediate (**TriOH**) was obtained by the reaction of 2 equiv of 2-mercaptoethanol with epichlorohydrin in the presence NaOH as a base (Scheme S1a). The reaction of **TriOH** and **TetraOH** with thiourea was followed by the base hydrolysis of the corresponding thiouronium salt yielding the multifunctional thiols **1b** and **1c** as colorless liquids in moderate (>65%) yield. Both monomers displayed viscosities of 43 and 189 cP and refractive index values (n_D/20 °C) of 1.636 and 1.647, respectively (Figure 1). As each alkyne functional group is difunctional (i.e., able to react twice), the simplest alkyne monomer **2a** used in this study was prepared in two high-yielding steps starting from the reaction of epichlorohydrin and thiophenol.[27] In the second step, deprotonation of the 2° alcohol **BPTP** was followed by alkylation with propargyl bromide and afforded low-viscosity (32 cP) **2a** in 91% yield with an accompanying refractive index value (n_D/20 °C) of 1.611. In contrast, the monomer **2b** with a viscosity of 14 cP and refractive index value (n_D/20 °C) of 1.591 was in turn prepared in a single step in 85% yield via the alkylation of dithiol **1a** with propargyl chloride in the presence of KOH as base (Scheme S1b).

The first step for the synthesis of the diyne monomers **2c** and **2d** involves the borax-catalyzed selective ring-opening reaction of epichlorohydrin with thiophenol (Scheme S1c). The reaction of epichlorohydrin with 1 equiv of thiophenol gave the chloro intermediate **CPTP** in excellent yield (>90%) as a colorless liquid. Further reaction of **CPTP** with a high refractive index dithiol "core" such as 1,2-ethane dithiol and 4,4′-thiobisbenzenethiol in the presence of a base yielded the corresponding alcohols **EDTOH** and **TBTOH**, respectively, in >90% yields. Following this strategy, any of the previously reported high refractive index multifunctional thiols can be used to fine tune the final material properties as per the need of the application under investigation.[40] Finally, the alkylation of these diols with 2 equiv of propargyl bromide yielded the respective dipropargyl ethers **2c** and **2d** in high overall yields of >65%. These two liquid monomers, **2c** and **2d**, had viscosity values of 171 and 732 cP, respectively, in addition to refractive index values (n_D/20 °C) of 1.603 and 1.668, respectively. Overall, the synthesis of these intermediates for both multifunctional thiols and diyne monomers is easily scaled up and stored for several months without any special precautions to be considered.

Photopolymerization and Real-Time FTIR Kinetics of Thiol−Yne Monomers. A generally accepted mechanism of the thiol−yne photopolymerization is shown in Scheme 1.

Scheme 1. Mechanism of the Radical-Mediated Thiol−Yne Click Reaction

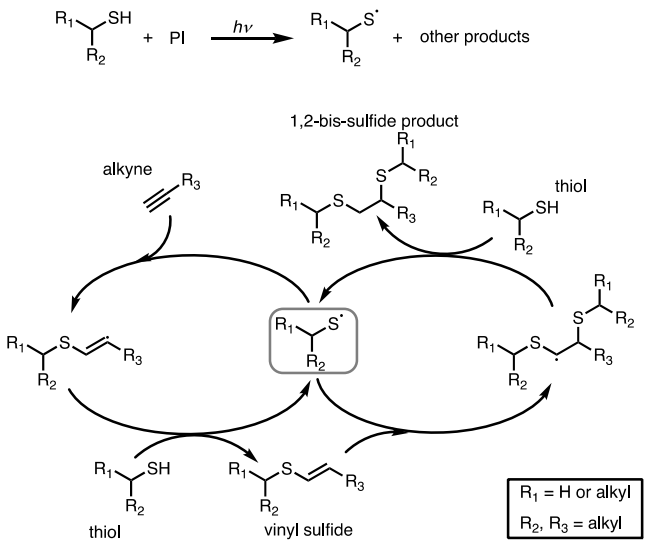

https://doi.org/10.1021/acsami.1c00831
ACS Appl. Mater. Interfaces 2021, 13, 15647−15658

Table 1. Physical and Optical Properties of Thiol−Yne-Based Photophotopolymer Networks

fomulation	thiol	yne	η (cP)[a]	n_D (589 nm)[b] polymer (resin)	n_D polymer − n_D resin	T_g (°C)	average strain at break (%)
A1	**1a**	**2a**	13	1.645 (1.606)	0.039	−33.8[c]	n/a
A2		**2b**	7	1.676 (1.596)	0.080	0	40.2
A3		**2c**	28	1.644 (1.601)	0.043	−18.0	13.9
A4		**2d**	71	1.669 (1.637)	0.032	−3.8	33.2
B1	**1b**	**2a**	26	1.649 (1.618)	0.031	−39.4[c]	n/a
B2		**2b**	20	1.682 (1.605)	0.077	19.2	20.5
B3		**2c**	71	1.655 (1.616)	0.039	−6.0	21.9
B4		**2d**	182	1.689 (1.647)	0.042	2.0	38.3
C1	**1c**	**2a**	64	1.648 (1.620)	0.028	−38.7[c]	n/a
C2		**2b**	52	1.683 (1.626)	0.057	11.1	17.6
C3		**2c**	209	1.654 (1.620)	0.034	−10.3	17.4
C4		**2d**	473	1.676 (1.646)	0.030	2.9	38.3

[a]Thiol−yne resins were formulated by mixing thiol and alkyne monomers in a 2:1 molar ratio of thiol:yne functional groups with ∼1 wt % TPO and were photopolymerized by irradiating with 405 nm LED light at 30 mW/cm^2. [b]Determined by rotational rheometry. [c]Refractive index is represented by the raunhofer D line (589 nm) [d]Determined by DSC.

Mechanistically, the radical-mediated thiol−yne reaction is analogous to that of the radical-mediated thiol−ene reaction in which each alkyne group reacts twice with thiyl radicals. The additional step involves the reaction of a vinyl sulfide intermediate formed in the first step with a second thiyl radical followed by a chain transfer to thiol to form another sulfide linkage. In kinetic analysis, each terminal alkyne group is considered difunctional, and therefore, to produce network polymers a minimum of two functionalities are required for both thiol and alkyne monomers.

In order to examine the photopolymerization kinetics, resin mixtures with stoichiometric thiol and alkyne (Yne:SH = 1:2) groups were formulated from the synthesized thiol and yne monomers (Table 1). All formulations formed miscible resin mixtures with low viscosities (<473 cP), and the conversions were monitored using real-time FTIR spectroscopy. Upon irradiation at 405 nm with an intensity of 30 mW/cm^2, both the thiol and the alkyne groups reacted quickly as indicated by the disappearance of the corresponding thiol (2570 cm^{-1}) and alkyne (2120 cm^{-1}) peaks. However, the reactivity of the thiol and alkyne were found to vary significantly with the steric and electronic nature of the monomers and also with resin viscosities to have a dramatic influence on the polymerization kinetics. For example, in formulations **A1**−**A4**, the monomer **1a** containing only a 1° thiol showed varying reactivities across the alkyne monomers **2a**−**2d**, indicative of the influence of viscosity and steric effects. Interestingly, the thiol and alkyne conversions for highly flexible diyne monomer **2b** and the monoyne **2a** reached up to 80% in 5 min as compared to the rest of the diyne monomers **2c** and **2d** for which the conversions reached only ∼70% (Figure 2a). This significant difference in the polymerization kinetics of **2b** is presumably due to the sterically less hindered backbone and its ability to form low-viscosity resin mixtures. However, the effect of secondary interactions such as $\pi-\pi$ stacking in diyne monomers **2a**, **2c**, and **2d** containing aryl groups cannot be ruled out. While all of the formulations containing **2b** showed high conversions of thiol as well as yne (∼80%), except for formulation **A1** which formed only linear polymers, the conversions were found to be significantly lower for all of the remaining formulations containing the yne monomers with aryl groups. This significant difference in conversions clearly shows the effects of steric hindrance and resin viscosities which upon network formation restrict the movement and hinder the accessibility of the thiol to react with the alkynes (Figure 2a−c). Moreover, in formulations containing **1a**, the higher concentration of vinyl sulfide in **A3** and **A4** compared to that of **A1** and **A2** clearly shows the inability of the thiols to react even with vinylsulfide, which is often several times more reactive than the corresponding alkynes (Figure S1a).[31] This inactivity of the vinyl sulfide in the system could be attributed to the steric hindrance induced after the reaction of one thiol. The reactivity of multifunctional thiols is highly influenced by the nature (i.e., 1° or 2°) and the relative position of the thiols. As expected the conversions were reduced to <80% for the formulations of **2b** with monomers **1b** and **1c** containing 2° thiols. As seen in the kinetic rate plots, the other yne monomers **2a**, **2c**, and **2d** containing bulky core structures reached a conversion of 60% or less in all cases (Figure 2b and 2c). This discrepancy was reasoned to be due to the restricted mobility and potentially lower reactivity of the shorter 2° thiol groups, which is difficult to access once the primary thiols of the same monomer have reacted. As pointed out previously, the increased steric hindrance of the 2° thiol increases the activation energy of the chain transfer step, resulting in a significantly reduced reaction rate. Though under lower initiation conditions, a similar trend in the reactivity of 1°, 2°, and 3° thiols was observed in thiol−ene photopolymer systems due to steric factors.[41,42] In order to better understand the reactivity of 2° thiols toward the alkynes, a model 2° thiol was synthesized following the general synthetic protocol (Figure S2). The reactivity difference of the alkyne toward 1° and 2° thiols was analyzed using hexanethiol (**HT**) and **3a** as model 1° and 2° thiols, respectively. The real-time FT-IR kinetics for formulations **M1** and **M2** containing stoichiometric **3a** and **HT** with **2a** (i.e., SH:Yne = 2:1) clearly show that the reaction rate of the 2° thiol is slower than that of the 1° thiol (Figure S3). Since the 2° thiol shares most of structural similarities with **1b** and **1c**, the lower conversion of the model 2° thiol clearly demonstrates that the steric bulk and the position has a significant influence on the thiol−yne reactivity. Although we were able to see that the peak corresponds to the unreacted thiol and yne in the FTIR spectra (Figure S5 in the SI), these monomers are less volatile and less harmful than aromatic thiols. Theoretically, the maximum extractable monomer even in the formulations with lower conversion (∼50%) (**B4** and **C4**) is only <6% (based on an equal probability of each functional group reacting). Also, in most

https://doi.org/10.1021/acsami.1c00831
ACS Appl. Mater. Interfaces 2021, 13, 15647−15658

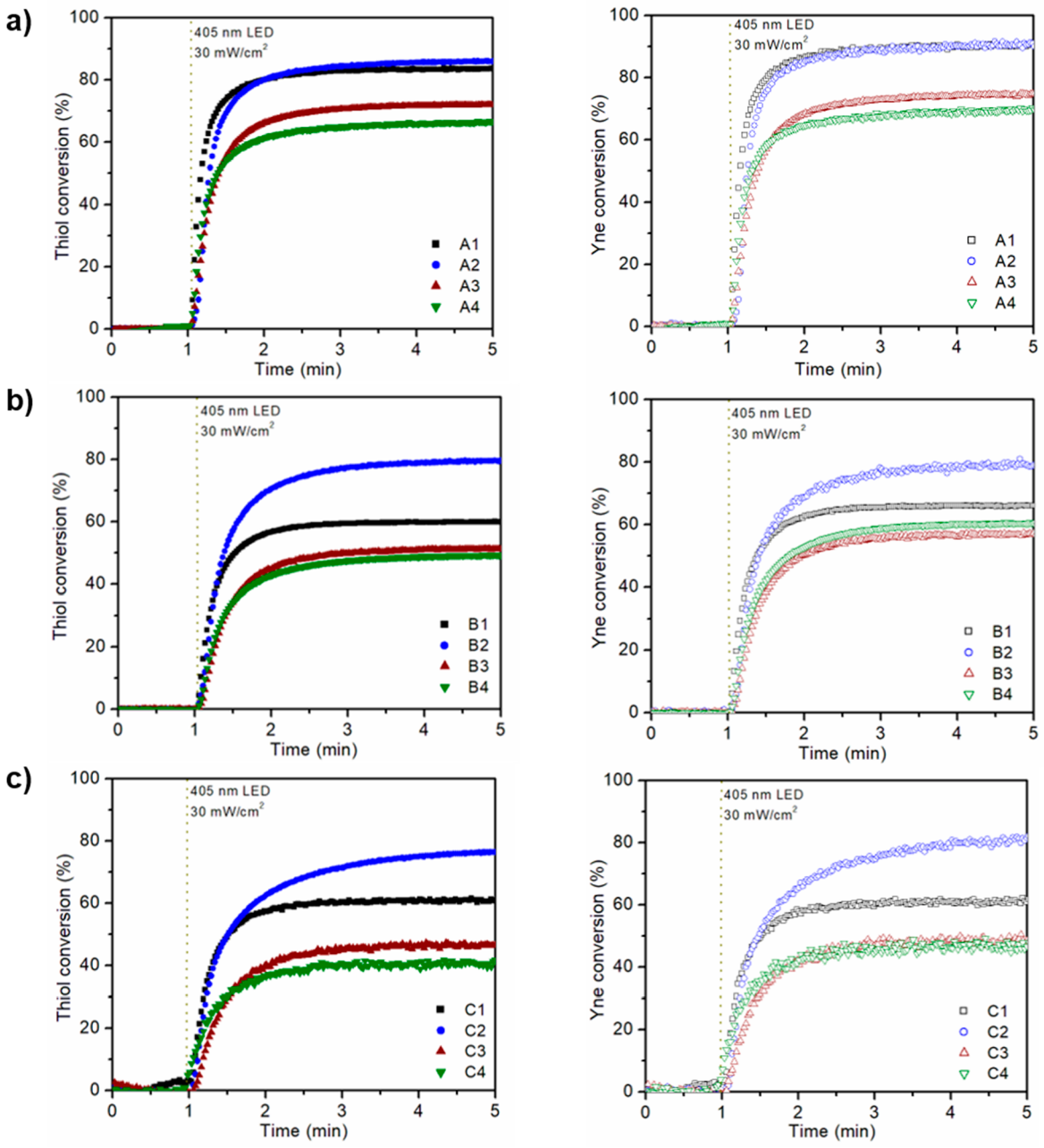

Figure 2. Real-time FTIR conversion vs time plots obtained for the resin formulation **A(1−4)** (a), **B(1−4)** (b), and **C(1−4)** (c). All of the resin formulations consisted of stoichiometric 2:1 thiol to alkyne functional group ratios. Each sample was stabilized in the dark for 1 min before irradiation with 30 mW/cm^2 405 nm wavelength at ambient temperature.

cases, the functional group conversion at a given time was found to be slightly higher for the alkyne than the thiol. This behavior is consistent with earlier observations that the addition of thiol to alkyne is significantly slower than the reaction between the thiol and the vinyl sulfide from which it was formed. Moreover, this difference may also be attributed to the consumption of alkyne or vinyl sulfide functional groups by chain growth homopolymerization.[32]

Photopolymerizations were also performed at an elevated temperature 60 °C (Figure S6) and at off-stoichiometric conditions (Yne:SH = 1:3) (Figure S7). Though a slight improvement in yne conversion was observed under off-stoichiometric conditions, no significant change in the conversion was observed at the elevated temperatures, indicating that the resin viscosity has little effect on the conversion and confirming the inability of the 2° thiol to participate efficiently in the reaction, even at elevated temperatures. Therefore, this study emphasizes that the choice of monomer based on the steric and electronic nature is crucial to achieve high reaction rates and conversions.

Thermomechanical Properties and Thermal Stability of High-*n* Thiol−Yne Photopolymers. One of the key features of the thiol−yne reaction over the analogous thiol−ene click reaction is that one alkyne reacts with two thiol moieties to give polymers with higher cross-link density than the corresponding thiol−ene formulations.[31] As mentioned above, all formulations formed completely miscible resin mixtures with low viscosities (<473 cP) and formed optically

https://doi.org/10.1021/acsami.1c00831
ACS Appl. Mater. Interfaces 2021, 13, 15647−15658

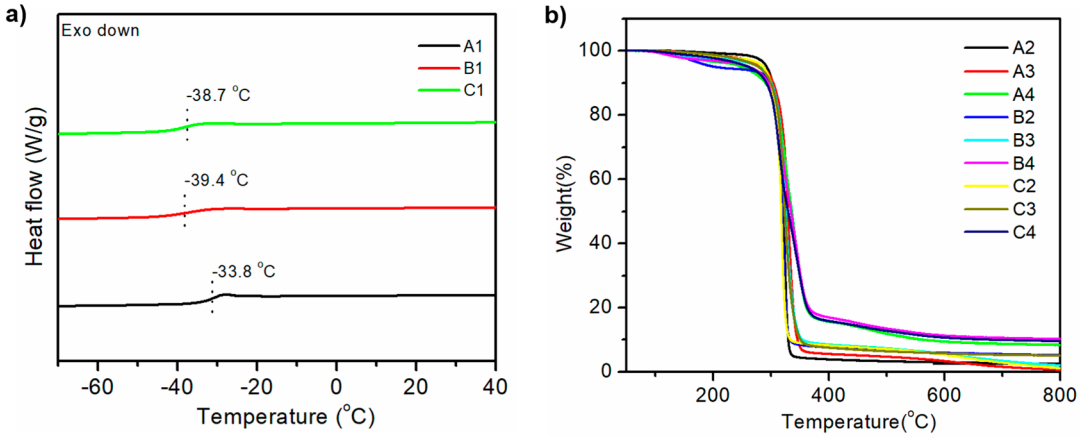

Figure 3. (a) DSC of the linear polymers obtained for formulations **A1**, **B1**, and **C1**. (b) TGA curves obtained for the formulation **A2**−**A4**, **B2**−**B4**, and **C2**−**C4**.

transparent films between the glass slides upon irradiating with 405 nm light at 30 mW/cm^2. Though the conversions were low particularly for the resin formulations containing diynes **2c** and **2d** with multithiols **1b** and **1c**, all of those were well above the gel point conversions and formed mechanically robust films (see Table S1 in the Supporting Information for the gel point conversions of all formulations used this study). Moreover, a lower gel point conversion than the Flory−Stockmayer prediction is observed for a stoichiometrically balanced, step-growth polymerization in which the ratio of the rate of initial addition to the subsequent addition is higher than unity (i.e., $kP,2/kP,1 > 1$).[31] One of the key features of the step-growth thiol−ene and thiol−yne networks is their rather narrow glass transition region resulting from the uniform network formation.[27] A similar trend was observed in the thiol−yne networks formed here, indicative of the relatively uniform network formation.[28] However, the tan δ curves obtained for the network formed from dithiol and diyne formulations were found to be somewhat broader compared to previously reported dithiol−diyne networks (Figure 3a−c). The reason for this discrepancy is believed to be nonuniform network formation due to the presence of two different thiol functionalities with different chemical environments as well as the difference in the reactivity of the alkyne and vinylsulfide intermediate. The presence of unreacted functionalities of various types in highly cross-linked systems is also expected to further diversify the relaxation times as indicated by broader tangent delta curves. All of the glass transition temperatures for the network polymers were measured by DMA except for formulations **A1**, **B1**, and **C1**, which were measured by DSC analysis due to the difficulty in large sample preparation (Figure 3a).

The glass transitions obtained for various thiol−yne formulations are listed in Table 1. As expected, the photopolymers obtained from formulations **A2**, **B2**, and **C2** exhibited higher T_g values between 0 and 19 °C in accordance with the higher conversions, whereas formulations **A1**, **B1**, and **C1** exhibited T_g below −30 °C due to the formation of mostly linear polymers with these formulations (see Figure S8 in the Supporting Information for representative SEC traces). However, an increase in T_g values was observed for all of the rest of the formulations containing diynes **2c** and **2d**. As expected, polymers **A4**, **B4**, and **C4** bearing the rigid thiobenzenethiol (TBT) core displayed higher T_g values (from −3.8 to 2.9 °C) compared to that of **A3**, **B3**, and **C3** bearing an ethane dithiol (EDT) core with T_g values in the range from −18 to −6 °C. Although the conversions of thiol and alkynes in these formulations were well above the gel point, the low overall conversions limit the expected cross-link density and T_g values. Thus, a broad range of thermomechanical properties was accessed for these photopolymer systems formed from diynes and multifunctional thiols with T_g values ranging from −18 to 19 °C and exhibited a similar transition from a glassy regime, where the elastic modulus is greater than 1 GPa, to a rubbery regime with a significantly lower modulus (Figure 4). Such high refractive index, low-T_g materials are suitable for optics and ophthalmic implant applications. The thermal stabilities of the photopolymers obtained from formulations **A2**−**A4**, **B2**−**B4**, and **C2**−**C4** were investigated by thermogravimetric analysis (TGA) under a nitrogen atmosphere (Figure 3b). The temperatures of 5% weight loss ($T_{d5\%}$) were found to be in the range of 320−335 °C for all of the polymers studied. Moreover, under uniaxial tensile loading, photopolymers **A2**−**A4**, **B2**−**B4**, and **C2**−**C4** strained at 10 mm/min at ambient conditions exhibited an average strain to break between 13% and 40% (Table 1).

Optical Properties of Thiol−Yne Photopolymers. As a result of the high inherent atomic refraction, sulfur-containing polymers are expected to exhibit high refractive indices. Therefore, the increase in the refractive index of the photopolymers formed from thiol-X polymerizations is a direct result of the incorporation of sulfide moieties into the network. One of the key features of thiol−yne photopolymerization is that it allows the introduction of a large number of sulfide linkages in comparison to that of the corresponding thiol−ene formulation. This unique feature of the thiol−yne reaction is attributed to the ability of one alkyne to react with two thiol groups, which is not possible for thiol−ene systems and results in the increased number of sulfurs in the system. Using this approach, photopolymers with large changes in refractive index was readily achieved by simply switching the monomer functionality from the vinyl to the corresponding alkyne reactive group. As can be seen from Table 1, each combination of synthesized thiol and yne monomers resulted in photopolymers with refractive indices n_D(20 °C) spanning a 0.04 range from approximately 1.65 to 1.69. These RI values at low conversions (~60%) are already higher than those reported earlier for analogous thiol−ene systems.[27] The high refractive

https://doi.org/10.1021/acsami.1c00831
ACS Appl. Mater. Interfaces 2021, 13, 15647−15658

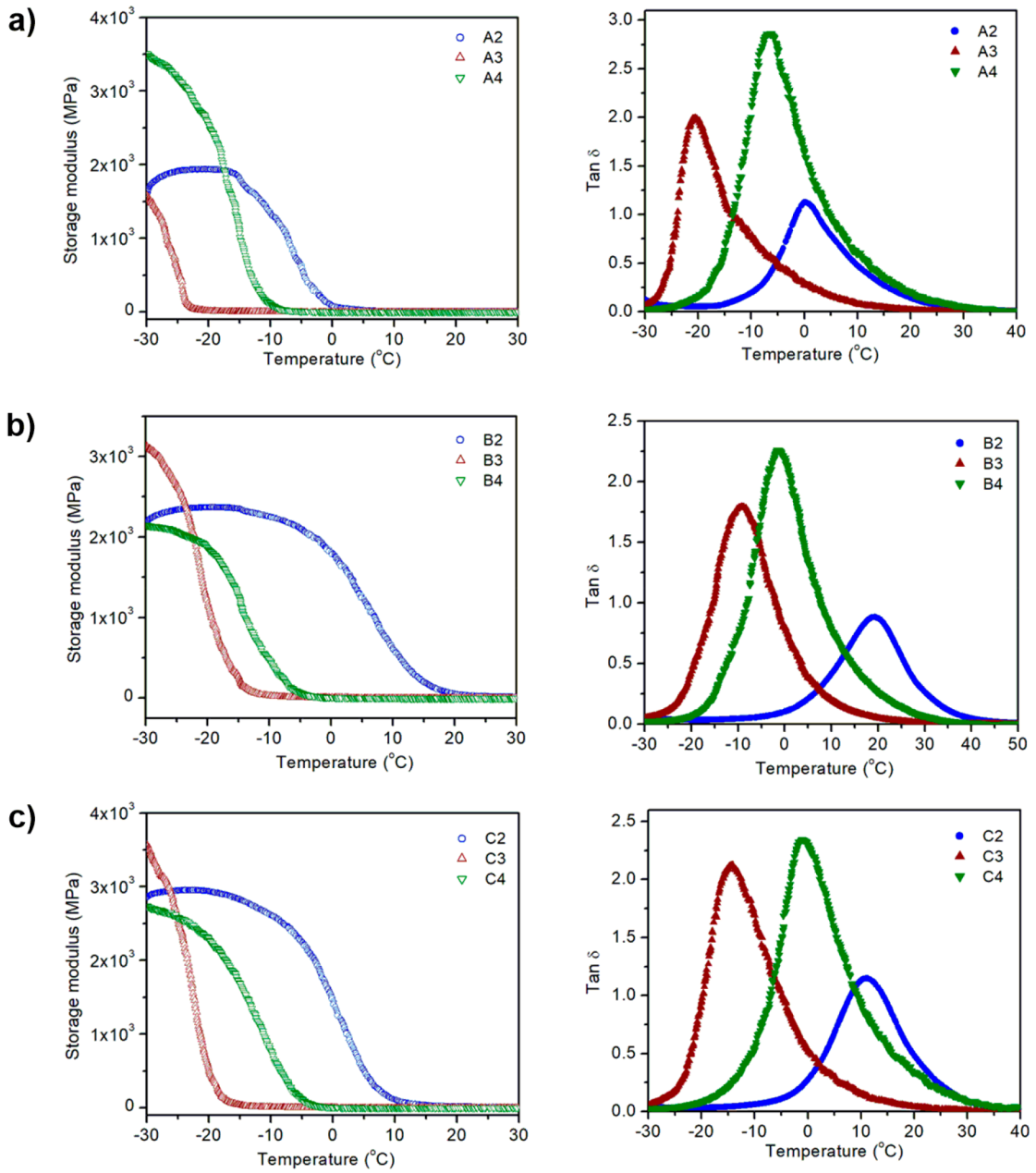

Figure 4. Thermomechanical properties of thiol−yne photopolymers obtained from formulations **A(2−4)** (a), **B(2−4)** (b), and **C(2−4)** (c). Storage modulus and tan δ plots as a function of temperature for each thiol−yne photopolymer film. DMA experiments were performed on the samples after postcuring overnight at 70 °C.

index values displayed by these network polymers are the direct result of the monomer core design incorporating substituents with high molar refraction. Thus, the aromatic dithiol core in **2d** significantly increases the refractive index by 0.03 compared to the alkyl counterpart **2c**. Using excess thiol, i.e., the off-stoichiometry in the resin formulation may improve the polymer refractive index as well as the conversion of the limiting reagent (i.e., yne monomer) by reducing the diffusional restrictions. However, an attempt to improve the polymer refractive index by off-stoichiometric combination of **1b** and **1c** across **2d** (thiol−yne, 3:1) impacted negatively, reducing the refractive index by 0.02. A plausible explanation for this discrepancy is that the free thiols contribute less to improve the refractive index in comparison to the thioether moieties resulting from the thiol−yne click reactions. This behavior is evident from the dramatic change in the refractive index (0.08) observed for formulation **B2** (thiol **1b** and yne monomer **2b**) during polymerization. Upon exposure to 405 nm light at 30 mW/cm^2 intensity, the refractive index of the resin changed from 1.60 to 1.68 in 5 min, indicative of the large number of thioether linkages formed due to the high conversion as well as the high intrinsic molar refraction of thioethers compared to that of the parent thiol (Figure S10). Since there are no aryl groups present in this resin system, the concentration of sulfide linkages gives a direct measure of the polymer refractive index. Interestingly, the measured polymer refractive index showed a linear relationship with the thiol conversion as shown in Figure 5.

While the majority of the photopolymers exhibited an optical transmittance of >85% at 500 nm for 250 μm thick

https://doi.org/10.1021/acsami.1c00831
ACS Appl. Mater. Interfaces 2021, 13, 15647−15658

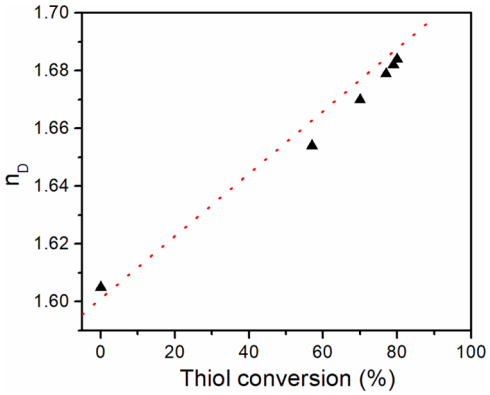

Figure 5. Plot of refractive index as a function of thiol conversion observed for formulation **B2** upon irradiation with 405 nm light, 30 mW/cm^2.

samples, the photopolymer **A2** with no aryl group displayed an even higher optical quality with transmittance as high as 93%, likely with a significant amount of the absorption due to the photoinitiator and its products (Figure 6).

Applications of High RI Thiol−Yne Monomers in a Two-Stage Photopolymer System. The ability of a photopolymer system to achieve high index contrast between the matrix and the writing monomers upon photoexposure is one of the key specifications for novel holographic material development. However, achieving such a high index contrast is often challenging due to limited availability of proper high RI monomers with low viscosities. To this end, Hata et al. utilized silica nanoparticle−polymer composites based on thiol−ene and thiol−yne photopolymers to achieve a high transparency and low shrinkage volume holographic recording with refractive index modulations of 0.01 and 0.008, respectively, for thiol−ene and thiol−yne systems.[43,44] Recently, Bowman and co-workers devised and implemented thiol−ene writing chemistry for high-fidelity hologram recording via a linear polyurethane binder approach.[45] Following a similar approach, these synthesized high RI alkyne monomers were used to record holograms with relatively high Δn in thin films. As seen from Figure 7a, a peak diffraction efficiency of 80% was achieved in high spatial frequency when **2d** and commercially available trimethylolpropane tris(3-mercaptopropionate (TMPTMP) were used as the writing monomers. The angular playback spectrum of the recorded hologram showed good

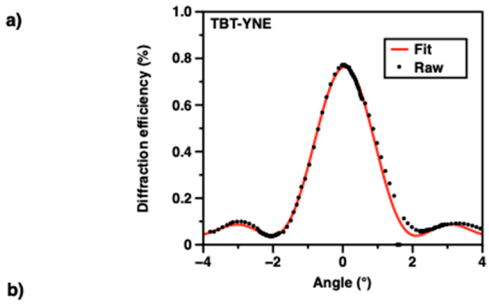

b)

Writing monomer	Thicknes (μm)	Dynamic range (Δn)	Haze (%)
2a	**14**	**0.013**	**0.74**
2c	**11**	**0.015**	**0.79**
2d	**11**	**0.018**	**1.24**

Figure 7. (a) Angular playback spectrum of a hologram recorded with **2d** as writing monomer showing a good fit to the coupled wave theory. (b) Summary of the dynamic ranges and haze measured for holograms with various alkyne writing monomers.

agreement with a fit to coupled-wave theory. Dynamic ranges (Δn) and thickness of holograms using the other alkyne writing monomers **2a** and **2c** are also summarized in Figure 7b. The hologram recorded with **2d** exhibits the highest Δn of 0.018 presumably due to the higher refractive index of this writing monomer formulation as compared to **2a** and **2c**. However, the diffusional blurring induced by the incomplete conversion of these writing monomers reduced the overall index contrast and remains a limitation in achieving high index modulation. Interestingly, the haze value measured for all of these holograms was found to be lower than 1.5%. A slightly higher haze observed for monomer **2d** is attributed to the low miscibility of this rigid core monomer with the urethane binder implemented here.

Another potential application of these photocurable thiol−yne resins is demonstrated by recording two-dimensional, micrometer-scale high refractive index structures on a poly(urethane−thiourethane) matrix. The model system demonstrated here consisted of a poly(urethane−thiourethane) matrix with high refractive index **B2** resin incorporated. The first-stage poly(urethane−thiourethane) matrix cured at ambient temperature was casted as a 250 μm thick

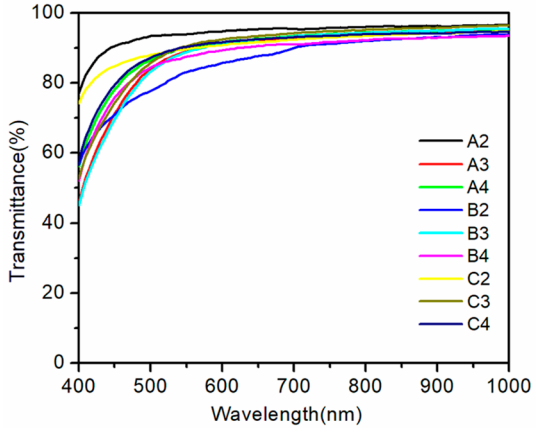

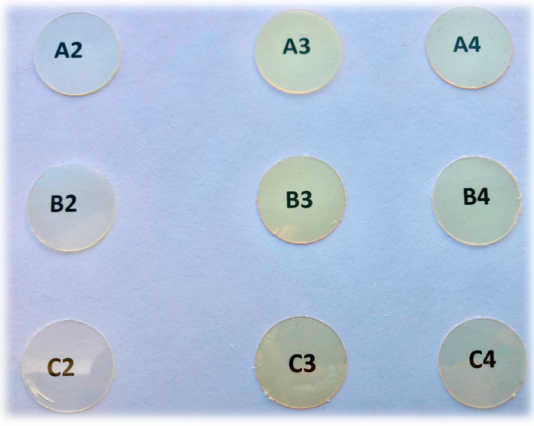

Figure 6. Optical transmittance and the picture of photopolymers **A2**−**A4**, **B2**−**B4**, and **C2**−**C4**.

https://doi.org/10.1021/acsami.1c00831
ACS Appl. Mater. Interfaces 2021, 13, 15647−15658

film between two glass slides. Upon exposure through a photomask using a 405 nm LED source, a two-dimensional array of refractive index structures (100 μm squares) was obtained as shown by the optical microscope image in Figure 8.

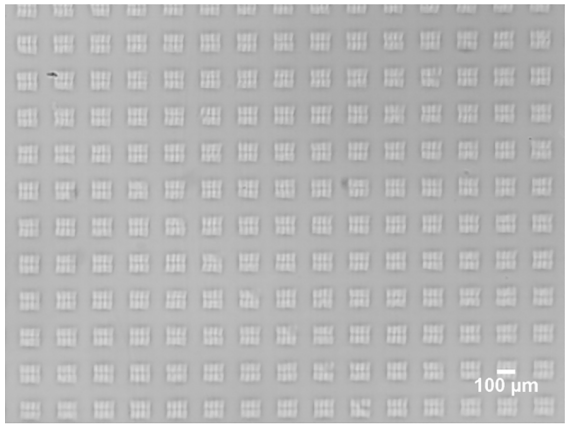

Figure 8. Illustration of two-dimensional, micrometer-scale refractive index structures recorded on a two-stage poly(urethane−thiourethane) matrix (Stage 1)/thiol−yne resin **B2** (stage 2) via irradiation through a photomask.

CONCLUSIONS

A scalable synthesis of multifunctional thiol and yne monomers with high intrinsic molar refraction has been successfully achieved from commercially available substrates. The monomers exhibited low viscosities (<500 cP) with refractive index values (n_D/20 °C) well above 1.6 and underwent photopolymerization via thiol−yne click reaction under ambient conditions in the presence of TPO as a photoinitiator upon exposure to 405 nm LED light with an intensity of 30 mW/cm^2 to form clear, optically transparent photopolymer films. The ability of the thiol−yne reaction to introduce a high concentration of sulfide linkages in the polymer network resulted in photopolymers with refractive index n_D(20 °C) values that exceed 1.68, significantly higher than that of the corresponding thiol−ene systems. In contrast to the thiol−ene system, steric bulk and reduced accessibility and reactivity of short-chain 2° thiols in the monomer design hampered monomer conversions resulting in a loosely cross-linked, low T_g material for materials with the secondary thiol. However, these issues are readily resolved using multifunctional thiols with no 2° thiol groups. Taking advantage of step-growth thiol−yne polymerizations, these monomers and photopolymers enable the design of new materials for a number of exciting optical applications.

ASSOCIATED CONTENT

Supporting Information

The Supporting Information is available free of charge at https://pubs.acs.org/doi/10.1021/acsami.1c00831.

General information, general experimental procedures, representative NMR spectroscopy (^{1}H and ^{13}C) of synthesized monomers (DOCX)

AUTHOR INFORMATION

Corresponding Author

Christopher N. Bowman − *Department of Chemical and Biological Engineering, Materials Science and Engineering Program, and BioFrontiers Institute, University of Colorado at Boulder, Boulder, Colorado 80309, United States;* orcid.org/0000-0001-8458-7723; Email: christopher.bowman@colorado.edu

Authors

Sudheendran Mavila − *Department of Chemical and Biological Engineering, University of Colorado at Boulder, Boulder, Colorado 80309, United States*

Jasmine Sinha − *Department of Chemical and Biological Engineering, University of Colorado at Boulder, Boulder, Colorado 80309, United States*

Yunfeng Hu − *Department of Chemical and Biological Engineering, University of Colorado at Boulder, Boulder, Colorado 80309, United States; Department of Chemistry, University of Colorado Boulder, Boulder, Colorado 80309, United States*

Maciej Podgórski − *Department of Chemical and Biological Engineering, University of Colorado at Boulder, Boulder, Colorado 80309, United States; Department of Polymer Chemistry, Institute of Chemical Sciences, Faculty of Chemistry, Maria Curie-Sklodowska University, Lublin 20-031, Poland*

Parag K. Shah − *Department of Chemical and Biological Engineering, University of Colorado at Boulder, Boulder, Colorado 80309, United States*

Complete contact information is available at: https://pubs.acs.org/10.1021/acsami.1c00831

Author Contributions

The manuscript was written through contributions of all authors. All authors have given approval to the final version of the manuscript.

Notes

The authors declare the following competing financial interest(s): A patent based on this work is pending.

ACKNOWLEDGMENTS

This work was supported by grants from Facebook K03 501401344 and the National Science Foundation CHE-1808484 grant.

REFERENCES

(1) Badur, T.; Dams, C.; Hampp, N. High Refractive Index Polymers by Design. *Macromolecules* **2018**, *51* (11), 4220−4228.

(2) Gaudiana, R. A.; Minns, R. A. High Refractive Index Polymers. *J. Macromol. Sci., Chem.* **1991**, *28* (9), 831−842.

(3) Higashihara, T.; Ueda, M. Recent Progress in High Refractive Index Polymers. *Macromolecules* **2015**, *48* (7), 1915−1929.

(4) Kleine, T. S.; Glass, R. S.; Lichtenberger, D. L.; Mackay, M. E.; Char, K.; Norwood, R. A.; Pyun, J. 100th Anniversary of Macromolecular Science Viewpoint: High Refractive Index Polymers from Elemental Sulfur for Infrared Thermal Imaging and Optics. *ACS Macro Lett.* **2020**, *9* (2), 245−259.

(5) Liu, J.-g.; Ueda, M. High Refractive Index Polymers: Fundamental Research and Practical Applications. *J. Mater. Chem.* **2009**, *19* (47), 8907−8919.

(6) Cheng, Y.; Lu, C.; Yang, B. A Review on High Refractive Index Nanocomposites for Optical Applications. *MATS* **2011**, *4* (1), 15−27.

(7) Macdonald, E. K.; Shaver, M. P. Intrinsic High Refractive Index Polymers. *Polym. Int.* **2015**, *64* (1), 6−14.
(8) Griebel, J. J.; Namnabat, S.; Kim, E. T.; Himmelhuber, R.; Moronta, D. H.; Chung, W. J.; Simmonds, A. G.; Kim, K.-J.; van der Laan, J.; Nguyen, N. A.; Dereniak, E. L.; Mackay, M. E.; Char, K.; Glass, R. S.; Norwood, R. A.; Pyun, J. New Infrared Transmitting Material via Inverse Vulcanization of Elemental Sulfur to Prepare High Refractive Index Polymers. *Adv. Mater.* **2014**, *26* (19), 3014−3018.
(9) Liu, J.-g.; Nakamura, Y.; Shibasaki, Y.; Ando, S.; Ueda, M. High Refractive Index Polyimides Derived from 2,7-Bis(4-aminophenylenesulfanyl)thianthrene and Aromatic Dianhydrides. *Macromolecules* **2007**, *40* (13), 4614−4620.
(10) Nakabayashi, K.; Imai, T.; Fu, M.-C.; Ando, S.; Higashihara, T.; Ueda, M. Poly(phenylene thioether)s with Fluorene-Based Cardo Structure toward High Transparency, High Refractive Index, and Low Birefringence. *Macromolecules* **2016**, *49* (16), 5849−5856.
(11) Su, Y.; Filho, E. B. D. S.; Peek, N.; Chen, B.; Stiegman, A. E. High Refractive Index Polymers (n > 1.7), Based on Thiol-Ene Cross-Linking of Polarizable P-S and P-Se Organic/Inorganic Monomers. *Macromolecules* **2019**, *52* (22), 9012−9022.
(12) Suzuki, Y.; Higashihara, T.; Ando, S.; Ueda, M. Synthesis and Characterization of High Refractive Index and High Abbe's Number Poly(thioether sulfone)s based on Tricyclo[5.2.1.02,6]decane Moiety. *Macromolecules* **2012**, *45* (8), 3402−3408.
(13) Tapaswi, P. K.; Choi, M.-C.; Jeong, K.-M.; Ando, S.; Ha, C.-S. Transparent Aromatic Polyimides Derived from Thiophenyl-Substituted Benzidines with High Refractive Index and Small Birefringence. *Macromolecules* **2015**, *48* (11), 3462−3474.
(14) Chen, X.; Liu, W.; Dong, B.; Lee, J.; Ware, H. O. T.; Zhang, H. F.; Sun, C. High-Speed 3D Printing of Millimeter-Size Customized Aspheric Imaging Lenses with Sub 7 nm Surface Roughness. *Adv. Mater.* **2018**, *30* (18), 1705683.
(15) Gissibl, T.; Thiele, S.; Herkommer, A.; Giessen, H. Two-photon Direct Laser Writing of Ultracompact Multi-lens Objectives. *Nat. Photonics* **2016**, *10* (8), 554−560.
(16) Beadie, G.; Shirk, J. S.; Rosenberg, A.; Lane, P. A.; Fleet, E.; Kamdar, A. R.; Jin, Y.; Ponting, M.; Kazmierczak, T.; Yang, Y.; Hiltner, A.; Baer, E. Optical Properties of a Bio-inspired Gradient Refractive Index Polymer Lens. *Opt. Express* **2008**, *16*, 11540−11547.
(17) Alim, M. D.; Glugla, D. J.; Mavila, S.; Wang, C.; Nystrom, P. D.; Sullivan, A. C.; McLeod, R. R.; Bowman, C. N. High Dynamic Range (Δn) Two-Stage Photopolymers via Enhanced Solubility of a High Refractive Index Acrylate Writing Monomer. *ACS Appl. Mater. Interfaces* **2018**, *10* (1), 1217−1224.
(18) Bruder, F.-K.; Facke, T.; Rolle, T. The Chemistry and Physics of Bayfol® HX Film Holographic Photopolymer. *Polymers* **2017**, *9*, 472.
(19) Bhagat, S. D.; Chatterjee, J.; Chen, B.; Stiegman, A. E. High Refractive Index Polymers Based on Thiol-Ene Cross-Linking Using Polarizable Inorganic/Organic Monomers. *Macromolecules* **2012**, *45* (3), 1174−1181.
(20) Chen, X.; Fang, L.; Wang, J.; He, F.; Chen, X.; Wang, Y.; Zhou, J.; Tao, Y.; Sun, J.; Fang, Q. Intrinsic High Refractive Index Siloxane-Sulfide Polymer Networks Having High Thermostability and Transmittance via Thiol-Ene Cross-Linking Reaction. *Macromolecules* **2018**, *51* (19), 7567−7573.
(21) Hoyle, C. E.; Bowman, C. N. Thiol-Ene Click Chemistry. *Angew. Chem., Int. Ed.* **2010**, *49* (9), 1540−1573.
(22) Hoyle, C. E.; Lowe, A. B.; Bowman, C. N. Thiol-click chemistry: a Multifaceted Toolbox for Small Molecule and Polymer Synthesis. *Chem. Soc. Rev.* **2010**, *39* (4), 1355−1387.
(23) McClain, C. C.; Brown, C. G.; Flowers, J.; Nguyen, V. Q.; Boyd, D. A. Optical Properties of Photopolymerized Thiol-Ene Polymers Fabricated Using Various Multivinyl Monomers. *Ind. Eng. Chem. Res.* **2018**, *57* (27), 8902−8906.
(24) Carioscia, J. A.; Lu, H.; Stanbury, J. W.; Bowman, C. N. Thiol-ene Oligomers as Dental Restorative Materials. *Dent. Mater.* **2005**, *21* (12), 1137−1143.
(25) Lu, H.; Carioscia, J. A.; Stansbury, J. W.; Bowman, C. N. Investigations of Step-growth Thiol-ene Polymerizations for Novel Dental Restoratives. *Dent. Mater.* **2005**, *21* (12), 1129−1136.
(26) Fang, L.; Sun, J.; Chen, X.; Tao, Y.; Zhou, J.; Wang, C.; Fang, Q. Phosphorus- and Sulfur-Containing High-Refractive-Index Polymers with High Tg and Transparency Derived from a Bio-Based Aldehyde. *Macromolecules* **2020**, *53* (1), 125−131.
(27) Alim, M. D.; Mavila, S.; Miller, D. B.; Huang, S.; Podgórski, M.; Cox, L. M.; Sullivan, A. C.; McLeod, R. R.; Bowman, C. N. Realizing High Refractive Index Thiol-X Materials: A General and Scalable Synthetic Approach. *ACS Materials Letters* **2019**, *1* (5), 582−588.
(28) Chan, J. W.; Zhou, H.; Hoyle, C. E.; Lowe, A. B. Photopolymerization of Thiol-Alkynes: Polysulfide Networks. *Chem. Mater.* **2009**, *21* (8), 1579−1585.
(29) Lowe, A. B.; Hoyle, C. E.; Bowman, C. N. Thiol-yne click chemistry: A Powerful and Versatile Methodology for Materials Synthesis. *J. Mater. Chem.* **2010**, *20* (23), 4745−4750.
(30) Chan, J. W.; Shin, J.; Hoyle, C. E.; Bowman, C. N.; Lowe, A. B. Synthesis, Thiol-Yne "Click" Photopolymerization, and Physical Properties of Networks Derived from Novel Multifunctional Alkynes. *Macromolecules* **2010**, *43* (11), 4937−4942.
(31) Fairbanks, B. D.; Scott, T. F.; Kloxin, C. J.; Anseth, K. S.; Bowman, C. N. Thiol-Yne Photopolymerizations: Novel Mechanism, Kinetics, and Step-Growth Formation of Highly Cross-Linked Networks. *Macromolecules* **2009**, *42* (1), 211−217.
(32) Fairbanks, B. D.; Sims, E. A.; Anseth, K. S.; Bowman, C. N. Reaction Rates and Mechanisms for Radical, Photoinitated Addition of Thiols to Alkynes, and Implications for Thiol-Yne Photopolymerizations and Click Reactions. *Macromolecules* **2010**, *43* (9), 4113−4119.
(33) Hoogenboom, R. Thiol-Yne Chemistry: A Powerful Tool for Creating Highly Functional Materials. *Angew. Chem., Int. Ed.* **2010**, *49* (20), 3415−3417.
(34) Yao, B.; Sun, J.; Qin, A.; Tang, B. Z. Thiol-yne Click Polymerization. *Chin. Sci. Bull.* **2013**, *58* (22), 2711−2718.
(35) Cook, A. B.; Barbey, R.; Burns, J. A.; Perrier, S. Hyperbranched Polymers with High Degrees of Branching and Low Dispersity Values: Pushing the Limits of Thiol-Yne Chemistry. *Macromolecules* **2016**, *49* (4), 1296−1304.
(36) Konkolewicz, D.; Gray-Weale, A.; Perrier, S. Hyperbranched Polymers by Thiol-Yne Chemistry: From Small Molecules to Functional Polymers. *J. Am. Chem. Soc.* **2009**, *131* (50), 18075−18077.
(37) Wei, Q.; Zan, X.; Qiu, X.; Öktem, G.; Sahre, K.; Kiriy, A.; Voit, B. High Refractive Index Hyperbranched Polymers Prepared by Two Naphthalene-Bearing Monomers via Thiol-Yne Reaction. *Macromol. Chem. Phys.* **2016**, *217* (17), 1977−1984.
(38) Rabiee, T.; Yeganeh, H.; Gharibi, R. Antimicrobial Wound Dressings with High Mechanical Conformability Prepared Through Thiol-yne Click Photopolymerization Reaction. *Biomed. Mater.* **2019**, *14*, 045007.
(39) Pötzsch, R.; Stahl, B. C.; Komber, H.; Hawker, C. J.; Voit, B. I. High Refractive Index Polyvinylsulfide Materials Prepared by Selective Radical Mono-addition Thiol-yne Chemistry. *Polym. Chem.* **2014**, *5* (8), 2911−2921.
(40) Okubo, T.; Kohmoto, S.; Yamamoto, M. Synthesis, Characterization, and Optical Properties of Polymers Comprising 1,4-Dithiane-2,5-bis(thiomethyl) Group. *J. Appl. Polym. Sci.* **1998**, *68* (11), 1791−1799.
(41) Cramer, N. B.; Reddy, S. K.; O'Brien, A. K.; Bowman, C. N. Thiol-Ene Photopolymerization Mechanism and Rate Limiting Step Changes for Various Vinyl Functional Group Chemistries. *Macromolecules* **2003**, *36* (21), 7964−7969.
(42) Long, K. F.; Bongiardina, N. J.; Mayordomo, P.; Olin, M. J.; Ortega, A. D.; Bowman, C. N. Effects of 1°, 2°, and 3° Thiols on Thiol-Ene Reactions: Polymerization Kinetics and Mechanical Behavior. *Macromolecules* **2020**, *53* (14), 5805−5815.
(43) Mitsube, K.; Nishimura, Y.; Nagaya, K.; Takayama, S.; Tomita, Y. Holographic Nanoparticle-polymer Composites Based on Radical-

https://doi.org/10.1021/acsami.1c00831
ACS Appl. Mater. Interfaces 2021, 13, 15647−15658

mediated Thiol-yne Photopolymerizations: Characterization and Shift-multiplexed Holographic Digital Data Page Storage. *Opt. Mater. Express* **2014**, *4*, 982−996.
(44) Hata, E.; Mitsube, K.; Momose, K.; Tomita, Y. Holographic Nanoparticle-polymer Composites Based on Step-growth Thiol-ene Photopolymerization. *Opt. Mater. Express* **2011**, *1*, 207−222.
(45) Hu, Y.; Kowalski, B. A.; Mavila, S.; Podgórski, M.; Sinha, J.; Sullivan, A. C.; McLeod, R. R.; Bowman, C. N. Holographic Photopolymer Material with High Dynamic Range (Δn) via Thiol-Ene Click Chemistry. *ACS Appl. Mater. Interfaces* **2020**, *12* (39), 44103−44109.

https://doi.org/10.1021/acsami.1c00831
ACS Appl. Mater. Interfaces 2021, 13, 15647−15658